

Rotating Shadowband Spectroradiometer Development and Spectral Shortwave Data Analysis Progress

J. Michalsky, L. Harrison, M. Qilong, J. Schlemmer, W. Berkheiser III, and J. Berndt
Atmospheric Sciences Research Center
University at Albany, State University of New York
Albany, New York

Introduction

Our principal goals in the Atmospheric Radiation Measurement (ARM) Program are high accuracy spectral irradiance measurements in the shortwave spectral region and the development and validation of techniques to retrieve climatologically important parameters based on these and other measurement at the Cloud and Radiation Testbed (CART) sites.

The principal instrument for spectral irradiance measurements in the shortwave spectrum in the ARM program is the multi-filter rotating shadowband radiometer (MFRSR). This instrument produces spectral irradiances in six 10-nm-wide bands, plus a broad-band measurement of total shortwave irradiance. This year we have developed methods for validating the basic filter measurements and improving the broad-band shortwave measurement made with a silicon cell sensor (Harrison et al. 1994).

These methods not only improve the basic quantities measured, but bolster the confidence we have in the retrievals obtained using the filtered data. This closure experiment will be demonstrated in this paper, and the improvement in aerosol retrieval will be illustrated. In the presence of uniform cloud cover, we have retrieved cloud optical depths and mean cloud particle radius using the MFRSR data and the microwave radiometer measurement of liquid water vapor.

Significant progress is reported in the development of the rotating shadowband spectroradiometer. This instrument will simultaneously measure spectral irradiance in 512 bands, spanning the range of approximately 360 to 1050 nm with spectral resolution of 0.6 to 8 nm, respectively.

Irradiance Measurements

The MFRSR is calibrated in the spectral channels using a NIST-traceable tungsten-halogen lamp that, if operated under specific conditions of power input and orientation, produces

known irradiances at a given distance from the lamp. Therefore, at the time of calibration, we can relate this spectral irradiance to a number of counts output by the data acquisition system.

In operation the MFRSR measures irradiance with a linear response according to the Bouguer-Lambert-Beer law given by

$$I = I_o e^{-\tau * m}$$

where I is the measure irradiance in counts, I_o is the irradiance that would be measured at the top of the atmosphere, τ is the total optical depth in the zenith direction, and m is the air mass relative to the zenith direction. If we linearize this equation by taking the natural logarithm of both sides and plot the $\ln(I)$ versus m , the slope τ is the total optical depth, and the intercept is the $\ln(I_o)$ for clear and stable atmospheric conditions.

With the retrieved I_o in counts multiplied by the calibration constant obtained from exposure to the lamp, we have an estimate of the extraterrestrial spectral irradiance, which can then be compared with standard tables of the extraterrestrial spectral irradiance for the particular filter response.

In Table 1, we show the results of this analysis for an MFRSR head calibrated and sent to Mauna Loa, Hawaii. Large errors outside the 4% error quoted for the lamp calibration were seen in four filters. Results obtained after the head was retrieved and recalibrated are shown in Table 2.

Table 1. Original calibration of MFRSR head for Mauna Loa.

Wavelength (nm)	414	499	608	663	858	936
I_o (Langley)	0.775	1.327	1.494	1.602	1.018	0.729
I_o (WMO)	1.78	1.91	1.76	1.57	0.994	0.820
% difference	-56	-31	-15	2	2	-11

Wavelength (nm)	406	494	608	663	858	936
I_0 (Langley)	1.17	1.97	1.80	1.55	0.986	0.854
I_0 (WMO)	1.67	1.94	1.74	1.56	0.956	0.836
% difference	2	2	3	-1	3	2

The filters near 415, 500, and 940 nm had shifted in wavelength because the interference filters had been bent by rough handling during shipment. The filter near 610 nm had actually degraded.

In Figure 1 the shift in the aerosol optical depths with the correct assignment of wavelength is especially significant, given the low optical depths for Mauna Loa aerosol. Most of this shift is caused by subtraction of a smaller Rayleigh scattering optical depth than was appropriate for the filter's actual passband. Retrieval of the ozone column improved with the bias error decreasing by 50%. The water vapor improvements were significant because the filter passband actually covered a very different portion of the water vapor band near 940 nm than originally measured.

Differences in AOD caused by Filter Shift

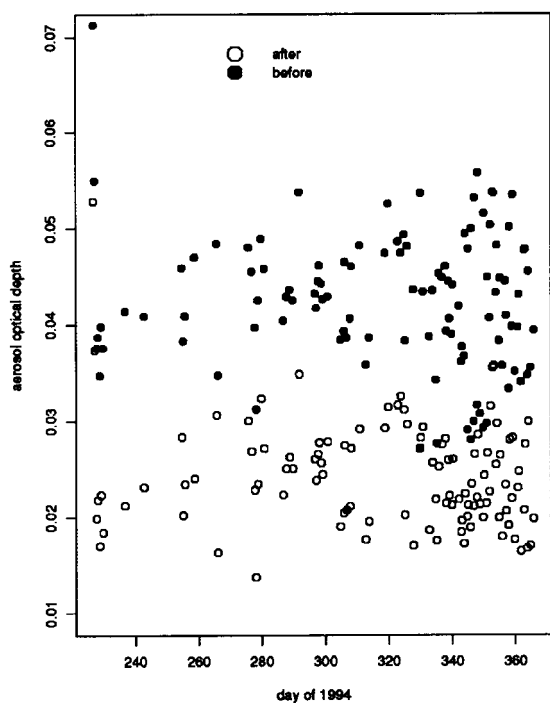


Figure 1. Differences in aerosol optical depth before and after filter correction.

Cloud Properties

We have developed an inversion method to infer the optical properties of clouds from the surface measurements using a nonlinear least squares retrieval based on an accurate and efficient adjoint method of radiative transfer. This retrieval assumes a homogeneous water cloud layer inserted in a vertical inhomogeneous, non-isothermal plane-parallel media. We show that these results are consistent with a simple delta-Eddington formulation, but superior in all cases, particularly those with lower optical depths. If the liquid water path (LWP) is available (e.g., from the multiwave radiometer) both the cloud optical thickness and effective radius can be retrieved. If the LWP is not available, the algorithm can provide an estimate of the cloud optical depth using a fixed effective radius; doing so increases the uncertainty of the retrieval by approximately 2% to 3%.

We compared our results with Geostationary Operational Environmental Satellite (GOES) measurements at the ARM Southern Great Plains (SGP) site during the spring intensive observation period (IOP) '94 (Minnis et al. 1995). Here, we show only one case on April 22. The inferred effective radii, shown in Figure 2, are typical of continental clouds (Han et al. 1994) and range from 6.1 μm to 14.7 μm with an average of 8.5 μm . The optical depths inferred from both a simple delta-Eddington model and our complex model with fixed $r_c = 10 \mu\text{m}$ are also shown in the bottom panel of Figure 2. The cloud optical depths vary from 6.6 to 74, with the average of 33, and peak before the local noon. The simple delta-Eddington model overestimates cloud optical depths for

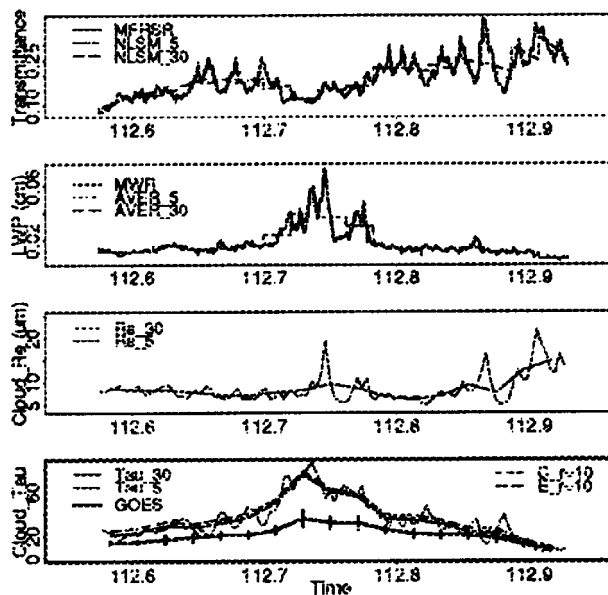


Figure 2. Retrieved cloud properties.

these observations by an average of 14%. The optical depths inferred from the complex model with fixed $r_c = 10 \mu\text{m}$ are within 3% of the results inferred when the LWP is used to also retrieve r_c . Our three surface retrieval methods produce optical depths substantially larger than the GOES retrievals, except late in the day when optical depths decline.

Overall, we retrieve effective radii with mean values of 11.3, 8.5, and 8.3 μm for April 5, 22, and 30, respectively. Temporal variations of the cloud optical depths are consistent between the surface and satellite measurements, and cloud optical depths agree well when the values are < 10 . However, at higher optical depths, the GOES results tend to be lower by as much as a factor of two compared with ours. This discrepancy is far too large to be explained by the estimated errors and uncertainties of the surface retrievals. The observed time-series of the data does not support spatial averaging by the satellite retrievals as the explanation because, above about 10, our cloud optical depths are always greater than GOES. We show that top-of-the-atmosphere measurements intrinsically have poor ability to distinguish among varying large optical depths and suggest that this bias may be general to the GOES retrievals. If so, then the satellite data (to which most existing climate models are tuned) substantially underestimate the optical depths for thicker low-altitude clouds.

Rotating Shadowband Spectroradiometer

The Rotating Shadowband Spectroradiometer (RSS) is a medium-resolution spectrometer used to measure terrestrial irradiance from 360 to 1050 nm. It consists of a prism spectrometer with a 512-element charge-coupled diode (CCD) array coupled to a rotating shadowband fore-optic. It uses the automated rotating shadowband technique to separate and measure the spectrally resolved direct, diffuse, and total horizontal spectral irradiances.

The dispersive optic of the RSS is a double-prism spectrograph; all optical elements are fused silica (synthetic amorphous quartz). All-quartz optics are used to permit observations below 400 nm. A prism spectrograph is advantageous (compared with a grating instrument) because it can achieve high (and uniform) throughput efficiency across the wide spectral range of the instrument. In addition, it is simple, and the optical elements are stable and rugged. The schematic of the instrument is shown in Figure 3.

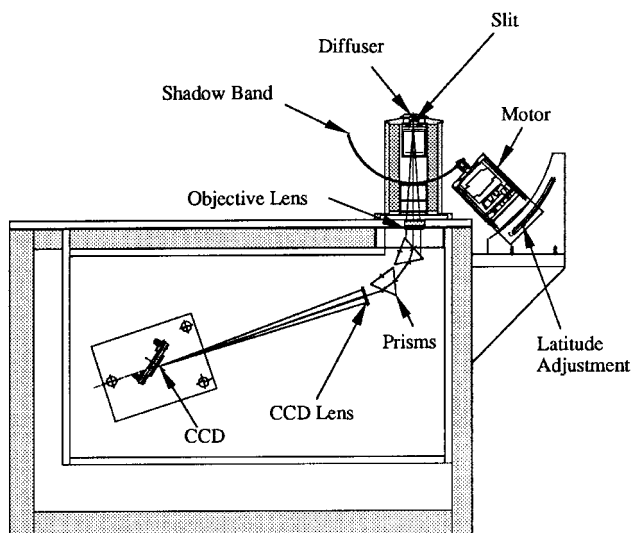


Figure 3. Rotating shadowband spectroradiometer schematic.

We can now operate the prototype RSS routinely as an automated shadowband instrument on our rooftop at the Atmospheric Sciences Research Center (ASRC). Sample data are shown in Figure 4. We are building two additional instruments that will incorporate improvements learned from the prototype testing. We plan to deploy one of these instruments at SGP for the late-summer H_2O IOP.

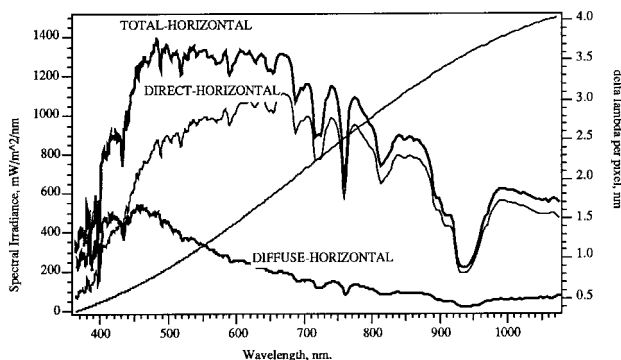


Figure 4. Total, diffuse, and direct horizontal for clear, hazy 16 November 1995.

References

Han, Q., W.B. Rossow, and A.A. Lacis, 1994: Near-global survey of effective droplet radii in liquid water clouds using ISCCP data, *J. Climate*, **7**, 465.

Harrison, L., J.J. Michalsky, and J. Berndt, 1994: The automated multi-filter rotating shadowband radiometer: An instrument for optical depth and radiation measurements, *Appl. Opt.* **32**, 5118-5125.

Minnis, P., W.L. Smith, D.P. Farber, J.K. Ayers, and D.R. Doelling, 1995: Cloud properties derived from GOES-7 for Spring 1994 ARM intensive observation period using version 1.0.0 of ARM satellite data analysis program, *NASA Reference Publication 1366*.